Shape Transitions of Epitaxial Islands during Strained Layer Growth: Anatase $TiO_2(001)$ on $SrTiO_3(001)$

Matthew S. J. Marshall and Martin R. Castell

Department of Materials, University of Oxford, Parks Road, Oxford, OX1 3PH, United Kingdom

(Received 26 August 2008; published 7 April 2009)

Extended annealing in UHV causes the surface region of $SrTiO_3(001)$ to become enriched with TiO_2, resulting in the formation of epitaxial islands of anatase $TiO_2(001)$. The islands are studied using UHV scanning electron microscopy (SEM), which reveals the changes in morphology during growth induced by misfit strain. Starting from a square island, two types of shape transition are observed. In the first, between 1000 and 1030 °C, the anatase islands elongate in length and narrow in width. This growth behavior follows the Tersoff-Tromp model [Phys. Rev. Lett. **70**, 2782 (1993)]. In the second growth mode, between 930 and 1000 °C, the islands relieve strain by the formation of trenches in the middle of each side of the square, thereby evolving into crosses. This shape arises because the lower annealing temperature imposes a kinetic constraint on the detachment of atoms necessary for island narrowing.

DOI: 10.1103/PhysRevLett.102.146102 PACS numbers: 68.35.Gy, 68.35.Fx, 68.37.Hk, 68.55.jm

Epitaxial islands are the active components in a variety of advanced devices such as single photon emitters [1,2] and quantum dot lasers [3,4]. Misfit strain between the islands and their substrates significantly influences the shape evolution of the islands as they increase their volume during growth. The strain can be relieved or partially relieved through the introduction of dislocations, but in metastable growth processes this is often avoided due to the high energetic cost of dislocation formation [5], for example, during the creation of dome-shaped Ge islands on Si substrates [6,7]. Alternative strain relief mechanisms include a shape transition during growth from a square island to a rectangular form. This process was studied by Tersoff and Tromp for Ag islands on a Si substrate, and a generalized model was developed that is applicable to islands that are kinetically limited to a constant height [8]. The shape transition occurs because the strain energy term in square islands increases more rapidly with volume than the surface and interface energy terms. For small volumes a square island is favored, but beyond a critical size the strain is reduced by elongation and narrowing. This model remains valid for systems where there is partial strain relief due to misfit dislocations and can explain shape transitions and the origin of high aspect ratio islands in numerous epitaxial growth systems ranging from semiconductors [9–13] to metals [14] and ceramics [15].

To accurately study the evolution of the shape of strained islands it is necessary to avoid interactions between neighboring islands. Such interactions include islands growing into each other, and the strained substrate of one island influencing its neighbor's growth. Interisland interactions are avoided by having widely spaced nucleation centers and growth that progresses in a manner that allows the islands to increase in volume without significant numbers of new islands being nucleated [8,11]. These criteria are satisfied during the process of TiO_2 surface segregation on $SrTiO_3$. When (001) oriented crystals of $SrTiO_3$ are annealed in a reducing atmosphere Ti and O segregate to the surface region, which becomes enriched in TiO_2 [16] and leads to the nucleation of epitaxial islands of anatase $TiO_2(001)$ [17]. The nucleation centers have a low density, but the supply of Ti and O atomic precursors diffusing on the surface allows unimpeded island growth. The small lattice mismatch of 3.1% between tetragonal anatase TiO_2 ($a = 3.784$ Å) and cubic perovskite $SrTiO_3$ ($a = 3.905$ Å) results in anatase islands that are under tensile stress. Molecular beam epitaxy (MBE) of titanium on $SrTiO_3(001)$ grown in an oxidizing atmosphere has also been effectively used to grow films of anatase-$TiO_2(001)$ on $SrTiO_3(001)$ but with a much higher nucleation density [18,19]. Here we report that at annealing temperatures from 1000 to 1030 °C the anatase islands follow the classic Tersoff growth behavior [8] of elongation and narrowing beyond a critical size. However, at temperatures ranging from 930 to 1000 °C a new process is observed: strain relief occurs through the creation of trenches within the islands which eventually leads to mature islands with cross shapes.

Single crystal epipolished $SrTiO_3$ samples were supplied by PI-KEM Ltd, UK, with (001) surface orientation and 0.5 wt % Nb doping. Doping is required so that the $SrTiO_3$ crystals are electrically conducting to enable experimental analysis and preparation. The samples were introduced into the ultrahigh vacuum (UHV) preparation chamber with a base pressure of 10^{-8} Pa. Samples were prepared by Ar^+ sputtering at an energy of 1.0 keV for a period of 10 min. This was followed by a 10 h anneal at 930 °C with subsequent anneals at temperatures ranging from 930 to 1030 °C by resistive direct current heating through the sample for an additional 10 h. Sample temperatures were measured through a viewport using a disappearing filament optical pyrometer. On a connected chamber there are facilities for UHV scanning electron microscopy (SEM) and Auger electron spectroscopy (AES). The SEM is a JEOL TM Z9043T operating at an

accelerating voltage of 12 kV. Atomic force microscopy (AFM) was performed in air using a Park Scientific Instruments Autoprobe CP.

Figure 1 shows typical examples of anatase islands at increasingly advanced stages of growth following UHV anneal temperatures in the range 1000–1030 °C. These islands are surrounded by dark depressions with a depth of 6.8 nm ± 2.0 nm as determined by AFM. Such depressions have also been observed around Ge islands grown on Si [20–22]. The islands initially grow as a square shape as shown in Fig. 1(a). Beyond a critical edge length of 1.3 μm the islands evolve into rectangular shapes with increased length and diminished width, shown in Fig. 1(b). This type of strain-induced shape evolution requires the anneal temperature to be high enough so that atomic detachment can occur at a sufficient rate to allow island narrowing. Ultimately, the islands become long thin rectangles with a width, α_0, which corresponds to the optimal value for the combination of strain relief and perimeter minimization. An island approaching this condition is shown in Fig. 1(c).

The strain and surface or interface energy per unit volume of the types of island shown in Fig. 1 is described by the following equation, formulated by Tersoff and Tromp [8]:

$$\frac{E}{V} = 2\Gamma\left(\frac{1}{s}+\frac{1}{t}\right)+\frac{1}{h}(\gamma_i+\gamma_t-\gamma_s) - 2ch\left[\frac{1}{s}\ln\left(\frac{s}{\phi h}\right)+\frac{1}{t}\ln\left(\frac{t}{\phi h}\right)\right], \quad (1)$$

where $\Gamma = \gamma_e \csc\theta - \frac{1}{2}(\gamma_t+\gamma_s-\gamma_i)\cot\theta$ and γ_e, γ_t, γ_s, γ_i are the edge, island top, substrate and interface energies, respectively. The island width is denoted by s and the length by t. The constant $c = \sigma_b^2(1-\nu)/2\pi\mu$, where μ, ν and σ are the shear modulus, Poisson's ratio and bulk stress, respectively, while $\phi = \cot\theta \exp(3/2)$ with θ defined as the angle between the island edge and the substrate. Minimizing the energy of an island of constant height with respect to both the length and width gives the optimal size of the island, where $s = t = \alpha_0$, and is given by

$$\alpha_0 = e\phi h \exp(\Gamma/ch). \quad (2)$$

The optimal size can be determined experimentally from the critical point, $e\alpha_0$, at which the shape transition from square to rectangle begins. Any partial relief of strain via misfit dislocations does not affect the validity of the model used to predict the shape transition but only reduces the effective value of the bulk stress σ_b.

In Fig. 2 the lengths (triangles) and widths (circles) of 130 anatase islands are plotted against their surface area. For areas below 1 μm^2 the vast majority of islands are square, hence the lengths and widths are the same, and lie on a parabola. Beyond 1 μm^2 some of the islands have assumed a rectangular shape; at 2 μm^2 the majority of islands are rectangular, and larger islands have an increasingly greater aspect ratio. The island heights were measured by AFM to be 30.8 nm with a ±4.0 nm standard deviation. The angle of the anatase side facets are determined by its crystallography to be 68°, and the average

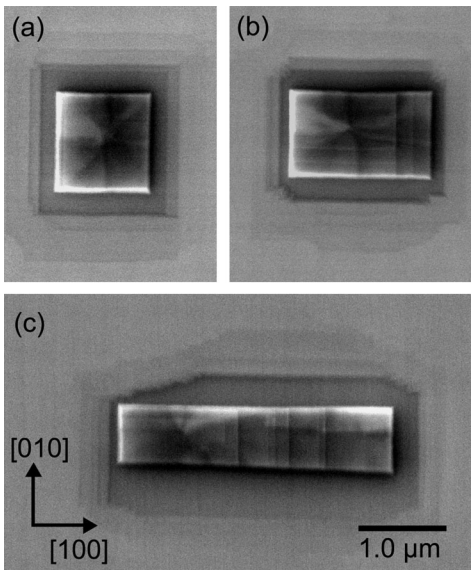

FIG. 1. Secondary electron UHV SEM images of anatase islands on $SrTiO_3$, which are formed at annealing temperatures between 1000 and 1030 °C. In (a) a square island is shown. Beyond a critical size the islands elongate and narrow, forming rectangles (b),(c).

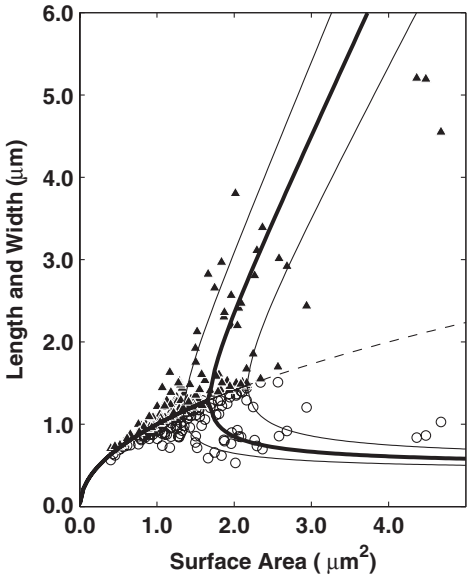

FIG. 2. Plot of anatase island lengths (solid triangles) and widths (open circles) versus surface area of the islands. The thick line represents the theoretically derived growth behavior of an island of average height 30.8 nm, with a bifurcation point at the critical width of 1.3 μm. The thin lines show the bounds due to the standard deviation of the island heights ±4.0 nm. The dashed parabolic line indicates how growth would proceed for unrelaxed islands. The error of measurement of individual data points is of the order of their size.

side length at which bifurcation occurs is 1.3 μm. This experimentally measured data can be used in Eq. (2) to calculate the ratio of materials constants $\Gamma/c = 1.25 \times 10^{-7}$ m. Previous STM studies have shown the anatase islands to exhibit a (4×1) reconstruction [17] whose surface energy was calculated to be $\gamma = 0.51$ J/m^2 [23,24]. A Wulff construction of the small islands can be used to determine a value for the composite surface energy term $\Gamma = 0.28$ J/m^2, and hence a value of $c = 2.3 \times 10^6$ J/m^3 can be calculated. It should be possible also to predict c via the elastic materials constants of anatase, but in practice this was not done due to the large discrepancies in the literature values by up to an order of magnitude [25–27]. Moreover, our value of c also takes account of the possibility of the partial relief of strain from misfit dislocations that may be introduced during the growth process.

Using the calculated values for the constants Γ and c derived previously, Eq. (1) can be used to calculate the optimum lengths and widths of islands as a function of surface area. The thick solid line in Fig. 2 shows the predicted dimensions of anatase islands of minimum energy with an average measured height of 30.8 nm. The thin lines either side of the thick line indicate the effect of the standard deviation of the island height ± 4.0 nm. Figure 2 shows sufficient agreement between theory and experiment for us to state that the growth of the anatase islands between 1000 and 1030 °C can be described by Tersoff's strained growth model [8].

When island growth is observed under similar conditions to that described above, but at lower temperatures between 930 and 1000 °C, the shape transition is dramatically different. Initial growth proceeds as a square island up to a critical area of 0.53 μm^2. Beyond this size a trench appears in the center of one of the sides of the square, as shown in Fig. 3(a). As growth proceeds, all sides develop trenches which grow towards the center of the island, but do not join up [Fig. 3(b)]. Mature islands have a cross shape where additional growth is at the tips of the branches, as shown in Fig. 3(c). *Ex situ* AFM of the islands reveals a representative average height of 22.5 nm with a standard deviation of ± 2.7 nm.

The data points in Fig. 4 show the perimeter of the islands grown at 930 °C versus their surface area. The perimeter is plotted, rather than length and width, because as the islands evolve into crosses lengths and widths can no longer be measured unambiguously. As also shown previously for the higher growth temperature, the islands are square up to a critical size and fall on a parabola. Beyond the critical area of 0.53 μm^2 trenches start to appear and hence the perimeter grows faster than the parabolic curve. Tersoff's growth model remains valid as a way of identifying the point at which the strain causes the square islands to become unstable and develop trenches. Hence, using Eq. (2) with an average experimentally determined critical side length of 0.73 μm, we can calculate that $\Gamma/c = 8.73 \times 10^{-8}$ m. This is used in conjunction with the previously derived value for $\Gamma = 0.28$ J/m^2, to calculate a value of $c = 3.21 \times 10^6$ J/m^3. Using these values of Γ and c the perimeter for a rectangular island with a measured height 22.5 nm can be calculated according to Eq. (1), and is shown as the thick line in Fig. 4. The thin lines on either side represent the differences in growth due to the standard deviation of the island heights of ± 2.7 nm.

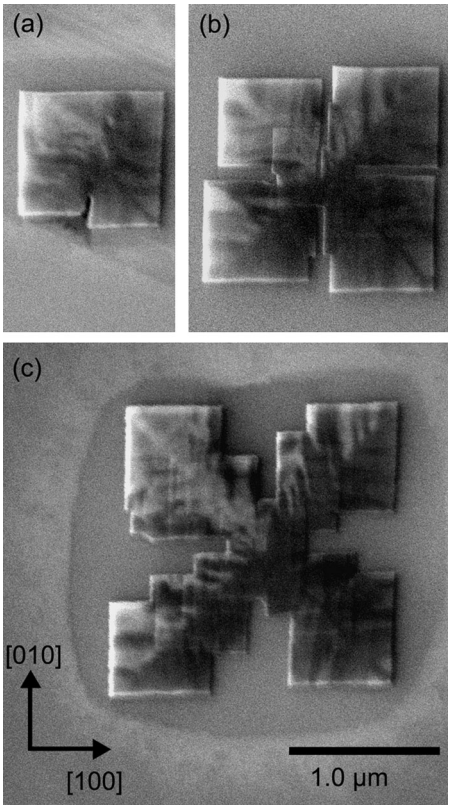

FIG. 3. UHV SEM images of anatase islands at various stages of growth formed at an anneal temperature of 930 °C. In (a) one side of the island forms a trench after the square reaches the critical size. In (b), another island is shown in which the shape transition has occurred, where the island symmetrically splits developing trenches in the middle of each of its four sides. Further annealing produces an island shape as shown in (c), which shows significant widening of the trenches and also shows growth from the tips of the cross.

Figure 4 allows a comparison to be made between the perimeter of the cross-shaped islands (triangle data points), the perimeter of a relaxed rectangle according to the Tersoff model (thick line), and unrelaxed square islands (dashed line). For perimeters exceeding 6.0 μm the cross-shaped island data points lie between the extremes of the relaxed and unrelaxed islands. This indicates that mature cross-shaped islands are more highly strained than their rectangular counterparts; i.e., the island in Fig. 3(c) is more strained than the island in Fig. 1(c).

We have shown that the shape transition of anatase islands on $SrTiO_3$ is dramatically affected by the anneal temperature at which the islands grow. This difference can be explained through the kinetics of the oxygen and tita-

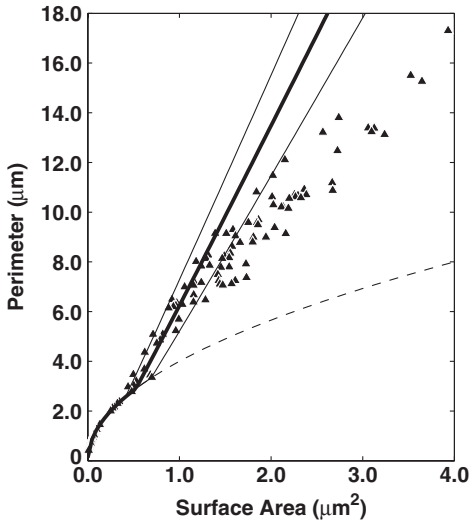

FIG. 4. Plot of island perimeters (triangles) versus their surface area for the types of island shown in Fig. 3. The thick line shows how growth would proceed according to Tersoff's model, Eq. (1), for a rectangular island of 22.5 nm height and a critical transition area of 0.53 μm^2. The thin lines correspond to the bounds due to the standard deviation in height of ± 2.7 nm. The dashed parabolic line shows unrelaxed island growth.

nium atomic precursors of the anatase islands. At temperatures between 1000 and 1030 °C the precursors continuously attach and detach from the islands. As growth proceeds, a shape transition that requires island narrowing into a rectangle can be achieved because atoms can detach from one side of the island and attach to another. Atomic detachment is less likely at temperatures between 930 and 1000 °C, with the consequence that island narrowing does not occur and strain is built up within the islands. Under these conditions the strain is relieved though an alternative mechanism involving the introduction of trenches which penetrate from the sides of the islands, as shown in Fig. 3(a). This trench formation mechanism allows strain relief to occur with a minimal amount of mass transport, as is appropriate for lower temperature growth. After trenches penetrate symmetrically from all four sides a cross-shaped island starts to evolve. This differs from another instance of 2D cross-shaped growth, in which increased adatom mobility at higher annealing temperatures allows strained films of Fe on W(001) to reform into crosses [28].

In summary, this Letter reports that epitaxial anatase islands on $SrTiO_3$ can undergo two types of shape transition, depending on the growth temperature. The first proceeds as predicted by Tersoff's theory [8]. The second occurs at lower temperatures and results in the formation of trenches as a strain relief mechanism. This leads to mature cross-shaped islands. This type of strain-induced shape transition has not been previously reported for epitaxial island growth. It illustrates that oxides and other ceramics may be subject to a variety of strained growth modes that are not found in metal and semiconductor systems, and we would expect to find island shape transitions similar to those reported here in other perovskites. Furthermore, synthesizing micron size crystals of anatase complements recent work done on freestanding similar-sized crystals by wet chemistry [29]. Our work also demonstrates that with an appropriate choice of substrate it is possible to synthesize micron-sized single crystal anatase islands with the highly reactive (001) face in UHV—providing a model system for studying its catalytic properties.

The authors would like to thank Chris Spencer (JEOL UK) for valuable technical support, and also David Newell and Nathan Cahill for many helpful discussions.

[1] P. Michler *et al.*, Science **290**, 2282 (2000).
[2] V. Zwiller *et al.*, Appl. Phys. Lett. **82**, 1509 (2003).
[3] L. Harris *et al.*, Appl. Phys. Lett. **73**, 969 (1998).
[4] D. L. Huffaker *et al.*, Appl. Phys. Lett. **73**, 2564 (1998).
[5] V. A. Shchukin and D. Bimberg, Rev. Mod. Phys. **71**, 1125 (1999).
[6] G. Medieros-Ribiero *et al.*, Science **279**, 353 (1998).
[7] F. M. Ross, R. M. Tromp, and M. C. Reuter, Science **286**, 1931 (1999).
[8] J. Tersoff and R. M. Tromp, Phys. Rev. Lett. **70**, 2782 (1993).
[9] W. Ma *et al.*, Appl. Phys. Lett. **79**, 4219 (2001).
[10] V. Zielasek, F. Liu, Y. Zhao, J. B. Maxson, and M. G. Lagally, Phys. Rev. B **64**, 201320(R) (2001).
[11] S. H. Brongersma, M. R. Castell, D. D. Perovic, and M. Zinke-Allmang, Phys. Rev. Lett. **80**, 3795 (1998).
[12] I. Goldfarb, Surf. Sci. **601**, 2756 (2007).
[13] W.-C. Yang, H. Ade, and R. J. Nemanich, J. Appl. Phys. **95**, 1572 (2004).
[14] B. Müller *et al.*, Phys. Rev. Lett. **80**, 2642 (1998).
[15] J. C. Nie, H. Yamasaki, and Y. Mawatari, Phys. Rev. B **70**, 195421 (2004).
[16] D. S. Deak *et al.*, J. Phys. Chem. B **110**, 9246 (2006).
[17] F. Silly and M. R. Castell, Appl. Phys. Lett. **85**, 3223 (2004).
[18] G. S. Herman and Y. Gao, Thin Solid Films **397**, 157 (2001).
[19] Y. Liang *et al.*, Phys. Rev. B **63**, 235402 (2001).
[20] X. Z. Liao *et al.*, Phys. Rev. B **60**, 15 605 (1999).
[21] S. A. Chaparro, Y. Zhang, and Jeff Drucker, Appl. Phys. Lett. **76**, 3534 (2000).
[22] I. Goldfarb, L. Banks-Sills, and R. Eliasi, Phys. Rev. Lett. **97**, 206101 (2006).
[23] M. Lazzeri, and A. Selloni, Phys. Rev. Lett. **87**, 266105 (2001).
[24] M. Lazzeri, A. Vittadini, and A. Selloni, Phys. Rev. B **63**, 155409 (2001).
[25] O. Zywitzki *et al.*, Surf. Coat. Technol. **180–181**, 538 (2004).
[26] V. Swamy and L. S. Dubrovinsky, J. Phys. Chem. Solids **62**, 673 (2001).
[27] J. K. Dewhurst and J. E. Lowther, Phys. Rev. B **54**, R3673 (1996).
[28] W. Wulfhekel *et al.*, Phys. Rev. B **68**, 144416 (2003).
[29] H. G. Yang *et al.*, Nature (London) **453**, 638 (2008).